

The Design of Stretch: A Compact, Lightweight Mobile Manipulator for Indoor Human Environments

Charles C. Kemp, Aaron Edsinger, Henry M. Clever and Blaine Matulevich

Abstract—Mobile manipulators for indoor human environments can serve as versatile devices that perform a variety of tasks, yet adoption of this technology has been limited. Reducing size, weight, and cost could facilitate adoption, but risks restricting capabilities. We present a novel design that reduces size, weight, and cost, while still performing a variety of tasks. The core design consists of a two-wheeled differential-drive mobile base, a lift, and a telescoping arm configured to achieve Cartesian motion at the end of the arm. Design extensions include a 1 degree-of-freedom (DOF) wrist to stow a tool, a 2-DOF dexterous wrist to pitch and roll a tool, and a compliant gripper. We justify our design with mathematical models of static stability that relate the robot’s size and weight to its workspace, payload, and applied forces. We also provide empirical support by teleoperating and autonomously controlling a commercial robot based on our design (the Stretch RE1 from Hello Robot Inc.) to perform tasks in real homes.

I. INTRODUCTION

Mobile manipulators for indoor human environments have the potential to serve as versatile devices that perform a variety of useful tasks. Examples from the literature include assisting people with disabilities [1]–[5], delivering medicine [5]–[7], cleaning [8]–[10], organizing [11]–[13], folding laundry [14]–[16], and entertaining [17], [18]. To date, mobile manipulators have primarily been used in robotics research labs. The long-imagined widespread use of mobile manipulators in homes and offices has yet to be realized, and use in controlled industrial spaces is nascent.

We posit that reduced size, weight, and cost will improve adoption of this emerging technology. Larger size increases a robot’s swept volume, limiting options for collision free navigation and manipulation. Greater mass worsens the consequences of collisions and falls. Larger and heavier robots are more difficult to manually move within an indoor space and transport between spaces. Higher cost reduces the feasibility of applications and increases the resources required to make copies of a robot, impeding adoption.

Our primary objective was to create a compact, lightweight, and affordable mobile manipulator capable of performing a variety of useful tasks within indoor human environments. Static stability becomes a dominant concern, since reducing weight and base size reduces the stably

Henry M. Clever is with the Georgia Institute of Technology (Georgia Tech), Atlanta, GA., USA. He was supported in part by NSF GRFP Grant DGE1148903. Aaron Edsinger and Blaine Matulevich are with Hello Robot Inc., Martinez, CA, USA. They were supported in part by NIH Award R43AG072982. Charles C. Kemp is with Georgia Tech and Hello Robot and is the corresponding author. He owns equity in and works part time for Hello Robot. He and Henry Clever receive royalties from Georgia Tech for sales of the Stretch RE1 due to a licensing agreement with Hello Robot. Pending patents cover parts of this paper.



Fig. 1. The Stretch RE1 mobile manipulator from Hello Robot Inc. provides a concrete example of our design. This image shows the Stretch RE1 handing an object to Dr. Aaron Edsinger in a real home.

achievable workspace and loads. Proportionally reducing the scale of an existing mobile manipulator reduces the set of feasible tasks, so we developed a novel design matched to indoor use with better scaling properties [19], [20].

To balance competing objectives, we used mechanical models and iterative design. For each iteration, we created a prototype robot and tested it with a variety of real tasks. From October 2016 to July 2017, we created and tested two prototype robots in the Healthcare Robotics Lab at Georgia Tech [21]. From August 2017 to May 2020, Hello Robot Inc. created a sequence of eight prototype robots with tests in a real home in Atlanta, Georgia, USA using teleoperative and autonomous control.

Robot	Width	Weight	Price
Stretch RE1 from Hello Robot	34 cm	23 kg	~\$20,000
HSR from Toyota [22]	43 cm	37 kg	N.A.
Fetch from Fetch Robotics [13]	51 cm	113 kg	~\$100,000
Tiago from PAL Robotics [23]	54 cm	70 kg	~\$58,000
PR2 from Willow Garage [24]	67 cm	227 kg	\$400,000

TABLE I

The resulting product, the Stretch Research Edition 1 (Stretch RE1), is significantly smaller, lighter, and less expensive than prior mobile manipulators with comparable capabilities (see Fig. 1 and Table I). Within this paper, we present the design of the Stretch RE1, justify the design with mathematical models of static stability, and provide empirical evidence that it can perform a variety of tasks in real homes.

II. THE DESIGN OF STRETCH

The Roomba robotic floor cleaner from iRobot served as an inspirational example for our design. By having a minimalist body well matched to the task of autonomously cleaning the floors of homes, the Roomba was widely adopted after its release in 2002 with over 1 million robots sold by October of 2004 [25]. Analogously, we wanted Stretch to have a minimalist design matched to mobile



Fig. 2. Stretch’s design has four main joints: a telescoping arm, a lift, and two drive wheels. **From left to right:** The Stretch RE1 with its arm retracted, extended, lowered, and raised. It is a right-handed robot.

manipulation in indoor human environments, much like the morphology of a well-adapted biological organism fit to its ecological niche [26], [27].

A. The Structure of Indoor Human Environments

Indoor human environments have Cartesian structure with horizontal planes and vertical surfaces, including floors, countertops, walls, doors, and cabinet faces. Humans have engineered these environments to facilitate comfortable perception, navigation, and manipulation by able-bodied people. Flat surfaces help objects remain in place. People often rest their bodies on approximately flat surfaces, such as the tops of beds and chair seats. Important locations tend to be accessible via clutter-free paths wide enough to walk through, and important objects tend to be visible from human head heights and reachable by human arms.

Pets and people, including children, older adults, and people with disabilities, are common occupants of indoor human environments, which creates challenges for safe operation. Falls, pinch points, high velocities, and high accelerations all present hazards. Motions that are difficult to predict can create challenges too, making it hard for pets and people to avoid risky situations. For example, knives, electrical outlets, and hinged doors represent common hazards, yet they are predictable and people learn to manage the risks.

Given these considerations, we created a statically stable wheeled robot with a small footprint that is tall enough to perceive and reach objects on elevated surfaces. Our design builds on prior work with the robot EL-E [28], which meets some of our criteria, but was too heavy (38.6 kg) and expensive (e.g., $\sim \$21,000$ for its 5-DOF Neuronics Katana arm) for widespread adoption.

B. Size and Weight

We developed the Stretch RE1 to work in homes, which tend to be more spatially constrained than indoor workplaces. Larger versions of Stretch might have applications outside of homes, such as in healthcare facilities and warehouses. The Stretch RE1 weighs 23 kg, which is above safety guidelines for a single person to lift [29], but light enough for a single person to roll or two people to lift. The length of the mobile base is 33 cm and it is 34 cm wide, which is the diameter of the first Roomba [30] and less than 50th percentile hip widths for adult females, 37.1 cm, and males, 36.1 cm [31]. Since all the robot’s components stow within the base’s footprint, its width is critical for navigation.

The head’s color camera is 131 cm above the ground when looking horizontally, which is between 50th percentile

sitting eye heights for adult females, 112.3 cm, and males, 121.9 cm, and 50th percentile standing eye heights for adult females, 151.4 cm, and males, 164.3 cm [31].

The bottom edge of the standard gripper’s closed fingertips reaches from the floor at 0 cm to 110 cm in height, so the full horizontal workspace covers the floor and standard 36-inch high countertops (≤ 92 cm). Most surfaces with frequent human interaction are near or below countertop height with significantly higher surfaces used for storage. The fingertips are 3.5 cm in diameter, so the center of the closed fingertips reaches 112 cm high, which is close to the 95th percentile right shoulder heights of female, 109.7 cm, and male, 113.4 cm, wheelchair users [32]. The outer edge of the closed fingertips reaches 71 cm out from the edge of the mobile base, which is similar to 50th percentile arm lengths for adult females, 67.3 cm, and males, 72.6 cm [31]. Additional reach can sometimes be achieved by moving the mobile base underneath surfaces, such as beds and tables.

C. The Four Main Joints

One of our key goals was to reduce the actuator requirements. Actuators influence the weight, complexity, and cost of robots. Each actuator requires power, signals, and control, and conventional electric motors with transmissions add significant weight, especially for proximal joints.

Stretch’s core design consists of four actuators that position the end of the arm within human environments (see Fig. 2). One actuator extends and retracts a horizontal telescoping arm, which is uncommon for mobile manipulators [33], [34]. The arm has a small cross section, reducing the mass and swept volume. Its linear motion is readily interpretable, such as when handing an object to a person. Another actuator moves the telescoping arm up and down a vertical mast, which we refer to as the lift. The mast also has a small cross section, which reduces mass and line-of-sight occlusion, and increases reach when the mobile base moves underneath a surface. The remaining two actuators drive the wheels of a conventional differential-drive mobile base to which the mast is mounted.

The horizontal telescoping arm is orthogonal to the forward motion of the mobile base. If we restrict the mobile base to forward and backward motion and assume no wheel slip, the end of the arm has Cartesian motion matched to the Cartesian structure of indoor human environments. Moving the mobile base forward and backward ($\pm q_m$) moves the end of the arm left and right ($\pm y_e$). The lift ($\pm q_l$) moves it up and down ($\pm z_e$), and the telescoping arm ($\pm q_a$) moves it out and in ($\pm x_e$). So, across the full workspace, $[x_e, y_e, z_e] = [q_a, q_m, q_l]$, the Jacobian is the identity matrix, I , and the manipulability ellipsoid is an axis-aligned sphere [35].

Without resorting to the complexities of nonlinear switching and underactuated dynamics, one can consider this to be a minimal configuration of actuators that produces Cartesian motion at the end of the arm and attains poses of the mobile base on the floor (2D position and 1D orientation). For example, removing the telescoping arm’s actuator would place a differential constraint on the motion of the end of the

arm, making it unable to move orthogonally to the forward motion of the mobile base. Removing the telescoping arm's actuator and instead making the mobile base omnidirectional with three actuators would achieve Cartesian motion of a fixed arm. However, a long fixed arm would increase the effective width of the robot, creating a hazard and limiting movement, while a short fixed arm would lose the benefits of a human-length cantilevered arm that can reach across surfaces.

When operating on flat floors, only the lift actuator works against gravity. The telescoping arm uses lightweight materials (e.g., carbon fiber) to achieve a long reach with low weight, reducing the lift actuator's requirements. The telescoping arm mounts to a carriage that passively resists moments due to the mass of the arm and applied loads, making the lift actuator's load consistent across arm configurations. The arm's lightweight structure also reduces its influence on the robot's center of mass (COM) when it is extended or raised.

D. Two Modes of Operation

While the four main joints move in various ways, it is conceptually helpful to consider two modes of operation: *navigation mode* and *manipulation mode*.

1) *Navigation Mode*: For the *navigation mode*, the telescoping arm retracts into the footprint of the mobile base and the robot drives around as a conventional differential-drive mobile robot. The lift can also lower the telescoping arm, lowering the robot's COM and increasing stability. In the navigation mode, the mobile base's forward direction of travel is considered the front of the robot and the direction of focus for sensors, perception, and human-robot interaction.

2) *Manipulation Mode*: For the *manipulation mode*, the front of the robot is the direction the telescoping arm extends, which is orthogonal to the mobile base's forward direction of travel. This mode provides Cartesian motion of the end of the arm, which we previously described. When the mobile base rotates in place, the telescoping arm rotates around a vertical axis near its proximal link, which is similar to rotation with a proximal shoulder joint at the base of a conventional serial manipulator. In addition to pure translations and rotations, the mobile base can perform curvilinear motions.

Notably, the mobile base plays a critical role in manipulation, since the lift and telescoping arm only position the end of the arm within a vertical plane. This contrasts with approaches to mobile manipulation that keep a mobile base stationary while manipulating with an arm. This is also distinct from approaches that mount a conventional serial manipulator to a mobile base. Our design uses an unconventional arm and a mobile base that work together.

3) *Mode Switching*: Often the robot uses the navigation mode to move to a task-relevant location and then switches to the manipulation mode. A challenge for human operators and autonomous control is to select a good location at which to make this transition. For example, if the goal is to grasp an object, the object should be within reach once the robot switches to the manipulation mode. The robot often rotates



Fig. 3. **Left:** Amazon product images for the ten grabbers we evaluated at Georgia Tech in May of 2017. The inset shows the top two. We converted the top left grabber into a robotic gripper. **Right:** Members of the Healthcare Robotics Lab evaluate grabbers by manipulating objects relevant to assistive robotics, including a pill and a utensil [36].

in place, lifts its arm, and extends its arm when transitioning from the navigation mode to the manipulation mode. It also rotates its head from looking in the forward direction of travel to looking toward the end-of-arm tool.

E. The Wrist and the Stretch Dex Wrist Accessory

The Stretch RE1 comes with a wrist yaw joint with a 330° range of motion that can stow a tool in the footprint of the mobile base without changing the tool's orientation with respect to gravity. In the navigation mode, the arm retracts and the wrist stows the tool. In the manipulation mode, the wrist swings the tool out, deploying it for use. Stowing tools in this manner makes the effective size of the robot smaller when navigating, avoiding collisions between the tool and the environment.

In addition to stowing the tool inside the footprint of the base, the wrist yaw joint provides task-relevant dexterity. It is a fifth DOF that adds dexterous redundancy to pure rotations of the mobile base. This is advantageous for manipulation on flat, horizontal surfaces. For example, it can rotate a camera to see behind objects on a shelf and orient the gripper to grasp elongated objects.

While the yaw joint is sufficient for a variety of tasks, some tasks benefit from additional degrees of freedom. The Stretch Dex Wrist is a recent accessory that adds a pitch joint followed by a roll joint in a serial chain. Together with the yaw joint, this results in a 3-DOF wrist and a 7-DOF robot.

The Dex Wrist enables tasks such as pouring and operating door knobs (see Fig. 7). It also increases the height the center of the closed fingertips can reach to approximately 130 cm above the ground, which is close to the 95th percentile right eye heights of female, 125.5 cm, and male, 127.0 cm, wheelchair users [32]. The pitch joint works against gravity, but is a distal joint with a relatively small moment arm that reduces demands on the actuator. In general, the four main joints provide gross movements over large distances, while the 3-DOF wrist and tools perform fine movements.

F. The Stretch Compliant Gripper

In May of 2017 at Georgia Tech, we developed a low-cost compliant gripper (see Fig. 3). Human-operated grabbers have long been used as affordable assistive devices to help people with disabilities reach and grasp objects in human

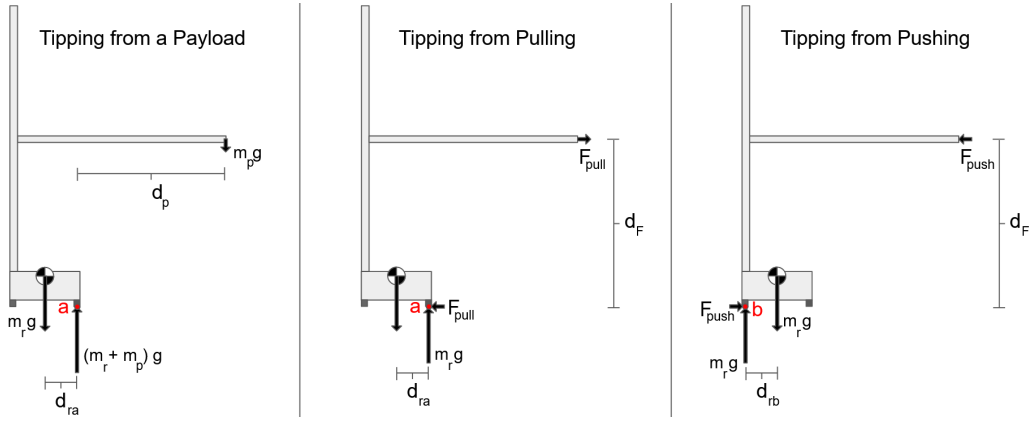


Fig. 4. Three free body diagrams (FBDs) showing planar models of tipping for task-relevant loads. The robot is in static equilibrium and all but one wheel is losing contact with the ground. Contact with the ground occurs at points *a* and *b* (shown in red) on the robot's right and left wheels, respectively.

environments. The grabbers are operated by pulling a cable that can be actuated [37].

To identify promising candidates, we used Amazon to find and purchase the highest-rated grabbers. Candidates had thousands of ratings and detailed reviews by people with disabilities. We purchased ten grabbers ranging from \$13.00 to \$33.95 in price with an average price of \$19.28.

We then conducted an informal evaluation to select the top candidates. We gathered objects relevant to assistive robotics, including objects from [36], and asked six lab members with expertise in assistive robotics to try the grabbers and choose their favorites (see Fig. 3). This process resulted in selection of the “Reacher Grabber by VIVE” and the “Japanese Reacher Grabber Pickup Tool”.

We found the rubber fingertips and spring steel flexures of the “Reacher Grabber by VIVE” to be highly capable and created a robotic prototype. The commercial version (Stretch Compliant Gripper) that comes with the Stretch RE1 provides kinematic and torque feedback from the actuator and can exert significantly more grip force than the original human-operated grabber, which is important for tasks such as operating door knobs. It also includes a mount point at a 90° angle with a hook useful for operating doors and drawers. The standard gripper tilts downwards, which permits grasping objects from above and from the side without use of a pitch joint. The Dex Wrist comes with a different version of this gripper that points straight out, since the Dex Wrist can both pitch and roll the gripper.

G. Stretch’s Sensors

The Stretch RE1 can sense applied loads with its actuators using current sensing. The four main joints have low gear ratios that facilitate this form of haptic sensing. The prismatic joints for the lift and arm enable straightforward contact detection, since their non-contact loads remain similar across configurations of the robot. Due to their sensitivity, the robot can autonomously open a variety of drawers by extending its arm until contacting the drawer’s surface, lowering its arm until contacting the handle, and then retracting (see Fig. 7).

The robot’s RGB-D camera (Intel RealSense D435i) is on a pan-tilt head with a 346° pan range of motion (ROM) and

a 115° tilt ROM. The head can pan to look in the direction of forward travel while navigating and at the end-of-arm tool while manipulating. It can also look straight down at its mobile base.

We rotated the camera 90° from its typical orientation to increase its vertical field of view (i.e., 87° for depth and 69° for color). This enables it to simultaneously obtain depth imagery from straight ahead and from the floor near the mobile base while navigating. It also gives it a fuller view of the arm’s workspace while manipulating. Panning the camera at a fixed downward tilt can capture a useful 3D representation of the surrounding environment, except for the region occluded by the mast. Viewing body-mounted ArUco markers on the mobile base, the wrist, and the proximal part of the arm supports kinematic calibration [38].

The robot has a laser range finder on its mobile base suitable for standard navigation methods. Only the mast occludes the laser range finder when the arm is raised. The robot has a microphone array on the top of the lift for speech recognition and sound source localization. The mobile base also has an inertial measurement unit (IMU) with rate gyros, accelerometers, and a magnetometer that can be used for navigation and tilt detection to avoid tipping and toppling [39]. The wrist has accelerometers that can be used for bump sensing, and the D435i has rate gyros and accelerometers useful for visual perception.

III. MODELING DESIGN TRADEOFFS

We used mechanical models of static stability to better understand key tradeoffs relating the robot’s size and weight to its capabilities in terms of workspace and loads.

A. Planar Models of Static Stability

Planar models that represent the robot just before it tips [40]–[42] highlight the design tradeoffs. These models assume the robot is in static equilibrium, such that all of the forces and moments cancel and the robot is perfectly balanced on a single wheel (see Fig. 4).

1) *Maximum Payload*: We first model the payload mass, m_p , that results in the robot being in static equilibrium balanced on its right wheel, *point a*. The moment due to the robot’s COM, $m_r d_{ra}$, and the moment due to the payload,

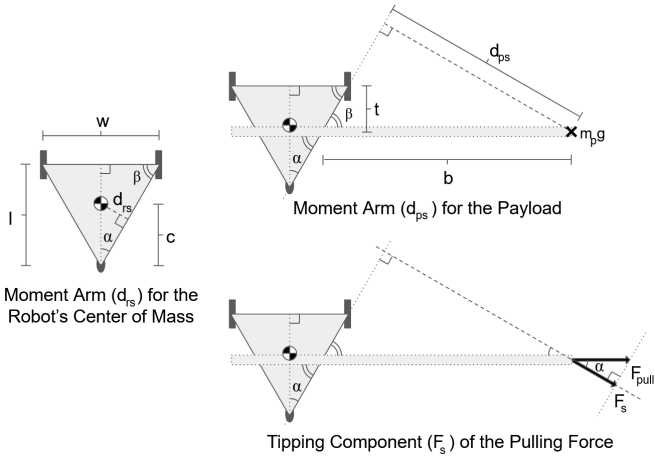


Fig. 5. Stretch's triangular support polygon changes stability under load.

$m_p d_p$, must sum to 0, implying $m_p = m_r \frac{d_{ra}}{d_p}$. Using the max reach beyond the right wheel, D , we find the max payload that results in static stability across the robot's full workspace, $m_{payload} = m_r \frac{d_{ra}}{D}$.

$m_{payload}$ is inversely proportional to the max reach, D , proportional to the mass of the robot, m_r , and proportional to the width of the mobile base, assuming the COM distance, d_{ra} , scales with the width of the mobile base. These relationships highlight key design tradeoffs, since we would like higher payloads, but also want the robot to be narrower, reach farther, and weigh less.

2) *Maximum Pulling & Pushing Forces*: We model the max pulling force, F_{pull} , assuming the moment due to the robot's COM, $m_r d_{ra}$, and the moment due to the pulling force, $F_{pull} d_F$, sum to 0, implying $F_{pull} = m_r g \frac{d_{ra}}{d_F}$.

The max pulling force is proportional to the mass of the robot, m_r , proportional to the width of the mobile base, and inversely proportional to the height of the arm, d_F . The robot can pull more strongly when its arm is low than when it is high. These relationships highlight additional design tradeoffs, since we would like higher pulling force, but also want the robot to be narrower, reach higher, and weigh less.

We model the max pushing force with $\sum M/a = F_{push} d_F - m_r g d_{rb} = 0$, implying $F_{push} = m_r g \frac{d_{rb}}{d_F}$. The main difference between F_{pull} and F_{push} is the moment arm for the robot's COM since $d_{ra} = w - d_{rb}$, where w is the width of the robot (i.e., the distance between the contact points for the two drive wheels). If the robot's COM is closer to its right wheel, $d_{rb} > d_{ra}$, then $F_{push} > F_{pull}$. If its closer to its left wheel, $d_{rb} < d_{ra}$, then $F_{push} < F_{pull}$. In practice, the configuration of the telescoping arm changes the lateral position of the robot's COM. For example, fully extending the arm reduces the max pulling force and increases the max pushing force (see Fig. 6).

B. Stability with a Triangular Support Polygon

Our planar model matches a mobile base with a rectangular support polygon, such as a base with two drive wheels and two passive casters. The Stretch RE1 uses a single passive omni wheel to help the drive wheels stay in contact when traversing thresholds and other uneven areas. This is similar

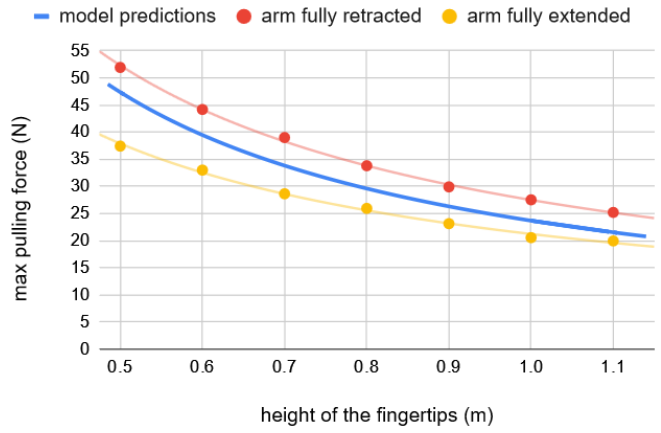


Fig. 6. Pulling force that tips the Stretch RE1. **Blue:** Model predictions. **Red:** Average measurements and fit curve with arm fully retracted. **Yellow:** Average measurements and fit curve with arm fully extended.

to the first Roomba. In practice, the Stretch RE1 tips over the sides of its support triangle formed by its three wheels.

During development, we updated our planar models to account for this difference (see Fig. 5). To simplify our analysis, we assume that the robot's COM is equidistant from the two drive wheels. The moment arm of the robot's COM becomes d_{rs} , which is the perpendicular distance to the left and right sides of the support triangle. $d_{rs} = c \sin \alpha$, where c is the distance from the robot's COM to the back wheel's point of contact and $\alpha = \arctan(\frac{w}{2l})$, where w is the width of the support triangle and l is its length.

The moment arm for the payload changes to d_{ps} . $d_{ps} = b \cos \alpha$, where $b = d_p + \frac{t}{\tan \beta}$, $\beta = \frac{\pi}{2} - \alpha$, and t is distance from the front side of the support triangle to the middle of the telescoping arm. As with our planar model, d_p represents the reach of the telescoping arm beyond the outer edge of the right front wheel (see Fig. 4). Brought together, $d_{ps} = (d_p + \frac{t}{\tan(\frac{\pi}{2} - \alpha)}) \cos \alpha$.

For pulling, only the component of the pulling force orthogonal to the side of the support triangle, F_s , plays a role, where $F_s = F_{pull} \cos \alpha$. Due to our simplifying assumption for the position of the robot's COM, this model results in the magnitude of the max pushing force being the same as the magnitude of the max pulling force. As with our planar model, d_F represents the height of the telescoping arm above the floor (see Fig. 4).

The resulting equations for the max payload across the entire workspace, $m_{payload}$, and the max magnitude of the pulling/pushing force, $F_{pull/push}$, as functions of the max reach of the robot's telescoping arm, D , and the height of the robot's telescoping arm, h , with $0 \leq h \leq H$ follow:

$$m_{payload} = m_r \frac{c}{t + \frac{2lD}{w}} \quad (1)$$

$$F_{pull/push} = m_r g \frac{cw}{2hl} \quad (2)$$

H , D , and W define the height, depth, and width of the robot's Cartesian workspace, $H \times D \times W$, given idealized forward and backward motion of the mobile base. W is effectively infinite under idealized conditions with unconstrained

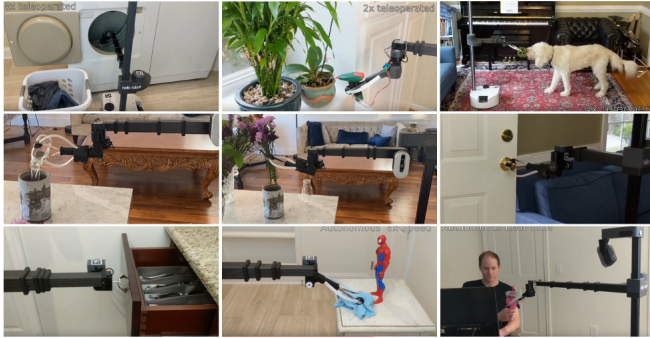


Fig. 7. Screenshots from task videos. **Top row:** Teleoperated. **Middle row:** Teleoperated with Stretch Dex Wrist. **Bottom row:** Autonomous.

motion. We also model the max force the robot can apply driving backwards, $F_{backpush} = m_r g \frac{(l-c)}{h}$, based on the height of the arm, h , and the moment arm for the robot's COM with respect to the front of the support triangle, $l - c$.

C. Other Design Considerations

A higher COM creates a greater risk of toppling due to high acceleration, bumps, thresholds, and ramps. The lightweight aluminum mast, carbon fiber telescoping arm, and small head reduce elevated mass, while the batteries and three of the four main actuators are located in the mobile base. The telescoping arm can also be lowered. When paused, the Stretch RE1 can be tilted over the two drive wheels to roll it around in a manner similar to an upright vacuum cleaner. This facilitates ease of use, but also increases the risk of toppling. Ignoring other factors, widening the mobile base by i cm increases the achievable full extension of the arm by $n i$ cm, where n is the number of telescoping elements.

D. Measurements & Model Predictions

To apply our models to the Stretch RE1, we used the centers of the wheels for the support triangle and balanced the robot on a metal cylinder to estimate the COM's location giving $w = 0.315$ m, $l = 0.24$ m, $m_r = 23$ kg, $g = 9.807 \frac{\text{m}}{\text{s}^2}$, and $c = 0.16$ m. Our derivations assumed the load was applied to the middle of the end of the arm. For our evaluation, we applied forces near the fingertips using a Nextech digital force gauge resulting in $H = 1.125$ m, $D = 0.6925$ m, and $t = 0.005$ m. Our models predict that $m_{payload} = 3.47$ kg, $F_{pull/push} = \frac{23.68 \text{ Nm}}{h}$ and $F_{backpush} = \frac{18.04 \text{ Nm}}{h}$.

We teleoperated a Stretch RE1 to a pose, measured the height of contact, h , and took five pulling force measurements. We used the gauge's hook to pull until the robot began to tip over. For the results in Figure 6, each circle shows the average of five measurements. Each group of five measurements had a standard deviation less than 1 N. Since our model assumes the COM is equidistant from the left and right sides of the support triangle, we made measurements with the arm fully retracted and fully extended.

We measured the max payload by teleoperating the robot to its max reaching distance, D , and pulling down with the gauge's hook until the robot began to tip over. The average of five measurements was 3.46 kg (SD of 0.065 kg), which closely matches our model's 3.47 kg prediction.

Tasks Performed by the Stretch RE1		
Task	Control	Date
Play with dog using a ball	local teleop	Feb 2020
Vacuum couch & floor	local teleop	Feb 2020
Wipe kitchen countertop	local teleop	Feb 2020
Move laundry from dryer to basket	local teleop	Feb 2020
Move toys from floor to box	local teleop	Feb 2020
Pickup pillows & place on couch	local teleop	Feb 2020
Hide plastic eggs for kids	local teleop	Feb 2020
Move toy chicken for kids to shoot	local teleop	Feb 2020
Water plants	local teleop	Feb 2020
Grasp objects from nightstand	autonomous	June 2020
Pull open drawers using haptic sensing	autonomous	July 2020
Wipe nightstand & avoid object	autonomous	July 2020
Hand object to person	autonomous	July 2020
Write HELLO on a whiteboard	autonomous	July 2020
Map, plan, navigate & reach a 3D point	autonomous	July 2020
Pick & place an object on a shelf	local teleop	July 2020
Inspect areas with a camera	local teleop	Dec 2020
Open an exterior door with a door knob	local teleop	Apr 2021
Pour water & place flowers in a vase	local teleop	June 2021

TABLE II

We confirmed that static stability limits the robot's capabilities by fixing the force gauge to the ground facing up and facing horizontally. We disabled the robot's force limits, retracted its arm, and teleoperated it to slowly apply loads. The robot pulled with > 70 N and lifted with > 60 N (> 6.12 kg). To avoid damage, we did not apply max forces.

Our results demonstrate that the measured force and payload capabilities of the Stretch RE1 meet requirements reported for assistive tasks. For example, drawers and cabinet doors required 20 N or less of pulling force to open [43], [44]. Face wiping and shaving required less than 10 N of pushing force [45]. Objects prioritized for retrieval by people with disabilities weighed less than 1.2 kg [36].

IV. TESTING THE DESIGN WITH A VARIETY OF TASKS

Table II lists full tasks we successfully performed with the Stretch RE1. Except for the inspection task, we performed all tasks in real homes. All of the code and full task videos (see Fig. 7) are publicly available on GitHub (<https://github.com/hello-robot>) and YouTube (<https://www.youtube.com/c/HelloRobot>). For local teleoperative control, an expert operator controlled the robot using a game controller. For autonomous control, the robot performed tasks using only its onboard sensors and computation.

Other researchers are beginning to disseminate their work with the Stretch RE1, providing further evidence for the efficacy of our design. For example, 21 people, including 3 people with disabilities, remotely operated the Stretch RE1 to perform kitchen tasks [46].

V. CONCLUSION

We presented a novel design for a lightweight, compact, lower cost mobile manipulator capable of performing a variety of tasks in indoor human environments. We supported our design with mechanical models and empirical results. The growing community using the commercially available Stretch RE1 suggests our design is increasing adoption of mobile manipulators. We are optimistic this community will help create a future in which mobile manipulators improve life for everyone.

REFERENCES

[1] K. A. Wyrobek, E. H. Berger, H. M. Van der Loos, and J. K. Salisbury, "Towards a personal robotics development platform: Rationale and design of an intrinsically safe personal robot," in *2008 IEEE International Conference on Robotics and Automation*. IEEE, 2008, pp. 2165–2170.

[2] T. L. Chen, M. Ciocarlie, S. Cousins, P. M. Grice, K. Hawkins, K. Hsiao, C. C. Kemp, C.-H. King, D. A. Lazewatsky, A. E. Leeper, *et al.*, "Robots for humanity: using assistive robotics to empower people with disabilities," *IEEE Robotics & Automation Magazine*, vol. 20, no. 1, pp. 30–39, 2013.

[3] P. M. Grice and C. C. Kemp, "In-home and remote use of robotic body surrogates by people with profound motor deficits," *Plos one*, vol. 14, no. 3, p. e0212904, 2019.

[4] J. S. Sefcik, M. J. Johnson, M. Yim, T. Lau, N. Vivio, C. Mucchiani, and P. Z. Cacchione, "Stakeholders' perceptions sought to inform the development of a low-cost mobile robot for older adults: A qualitative descriptive study," *Clinical nursing research*, vol. 27, no. 1, pp. 61–80, 2018.

[5] M. J. Johnson, M. A. Johnson, J. S. Sefcik, P. Z. Cacchione, C. Mucchiani, T. Lau, and M. Yim, "Task and design requirements for an affordable mobile service robot for elder care in an all-inclusive care for elders assisted-living setting," *International Journal of Social Robotics*, vol. 12, no. 5, pp. 989–1008, 2020.

[6] A. Prakash, J. M. Beer, T. Deyle, C.-A. Smarr, T. L. Chen, T. L. Mitzner, C. C. Kemp, and W. A. Rogers, "Older adults' medication management in the home: How can robots help?" in *2013 8th ACM/IEEE International Conference on Human-Robot Interaction (HRI)*. IEEE, 2013, pp. 283–290.

[7] M. Swangnetr, B. Zhu, K. B. Taylor, and D. B. Kaber, "Assessing the effects of humanoid robot features on patient emotion during a medicine delivery task," in *Proceedings of the Human Factors and Ergonomics Society annual meeting*, vol. 54, no. 4. SAGE Publications Sage CA: Los Angeles, CA, 2010, pp. 349–353.

[8] S. Elliott, Z. Xu, and M. Cakmak, "Learning generalizable surface cleaning actions from demonstration," in *2017 26th IEEE International Symposium on Robot and Human Interactive Communication (RO-MAN)*. IEEE, 2017, pp. 993–999.

[9] M. Cakmak and L. Takayama, "Towards a comprehensive chore list for domestic robots," in *2013 8th ACM/IEEE International Conference on Human-Robot Interaction (HRI)*. IEEE, 2013, pp. 93–94.

[10] G. Garcia Ricardez, N. Koganti, P.-C. Yang, S. Okada, P. Uriguen Eljuri, A. Yasuda, L. El Hafi, M. Yamamoto, J. Takamatsu, and T. Ogasawara, "Adaptive motion generation using imitation learning and highly compliant end effector for autonomous cleaning," *Advanced Robotics*, vol. 34, no. 3-4, pp. 189–201, 2020.

[11] S. Srinivasa, D. Ferguson, C. J. Helfrich, D. Berenson, A. Collet, R. Diankov, G. Gallagher, G. Hollinger, J. Kuffner, and M. V. Weghe, "Herb: a home exploring robotic butler," *Autonomous Robots*, vol. 28, no. 1, pp. 5–20, 2010.

[12] N. Blodow, L. C. Goron, Z.-C. Marton, D. Pangercic, T. Rühr, M. Tenorth, and M. Beetz, "Autonomous semantic mapping for robots performing everyday manipulation tasks in kitchen environments," in *2011 IEEE/RSJ International Conference on Intelligent Robots and Systems*. IEEE, 2011, pp. 4263–4270.

[13] M. Wise, M. Ferguson, D. King, E. Diehr, and D. Dymesich, "Fetch and freight: Standard platforms for service robot applications," in *Workshop on autonomous mobile service robots*, 2016.

[14] S. Miller, J. Van Den Berg, M. Fritz, T. Darrell, K. Goldberg, and P. Abbeel, "A geometric approach to robotic laundry folding," *The International Journal of Robotics Research*, vol. 31, no. 2, pp. 249–267, 2012.

[15] D. Seita, N. Jamali, M. Laskey, A. K. Tanwani, R. Berenstein, P. Baskaran, S. Iba, J. Canny, and K. Goldberg, "Deep transfer learning of pick points on fabric for robot bed-making," *arXiv preprint arXiv:1809.09810*, 2018.

[16] D. Estevez, J. G. Victores, R. Fernandez-Fernandez, and C. Balaguer, "Enabling garment-agnostic laundry tasks for a robot household companion," *Robotics and Autonomous Systems*, vol. 123, p. 103330, 2020.

[17] J. Bohren, R. B. Rusu, E. G. Jones, E. Marder-Eppstein, C. Pantosaru, M. Wise, L. Mösenlechner, W. Meeussen, and S. Holzer, "Towards autonomous robotic butlers: Lessons learned with the pr2," in *2011 IEEE International Conference on Robotics and Automation*. IEEE, 2011, pp. 5568–5575.

[18] R. Kittmann, T. Fröhlich, J. Schäfer, U. Reiser, F. Weißhardt, and A. Haug, "Let me introduce myself: I am care-o-bot 4, a gentleman robot," in *Mensch und Computer 2015–Tagungsband*. De Gruyter, 2015, pp. 223–232.

[19] D. W. Thompson and D. W. Thompson, *On growth and form*. Cambridge university press Cambridge, 1942, vol. 2.

[20] T. A. McMahon and J. T. Bonner, *On size and life*, 1983, no. Sirsi i9780716750000.

[21] T. Bhattacharjee, H. M. Clever, J. Wade, and C. C. Kemp, "Multimodal tactile perception of objects in a real home," *IEEE Robotics and Automation Letters*, vol. 3, no. 3, pp. 2523–2530, 2018.

[22] K. Hashimoto, F. Saito, T. Yamamoto, and K. Ikeda, "A field study of the human support robot in the home environment," in *2013 IEEE Workshop on Advanced Robotics and its Social Impacts*. IEEE, 2013, pp. 143–150.

[23] J. Pages, L. Marchionni, and F. Ferro, "Tiago: the modular robot that adapts to different research needs," in *International workshop on robot modularity, IROS*, 2016.

[24] S. Cousins, "Willow garage retrospective [ros topics]," *IEEE Robotics & Automation Magazine*, vol. 21, no. 1, pp. 16–20, 2014.

[25] iRobot, "iRobot's Roomba Robotic Floorvac Surpasses 1 Million in Sales," Available at investor.irobot.com/news-releases/news-release-details/irobots-roomba-robotic-floorvac-surpasses-1-million-sales (2021/09/14), 2004.

[26] R. A. Brooks, "How to build complete creatures rather than isolated cognitive simulators," in *Architectures for intelligence*. Psychology Press, 2014, pp. 239–254.

[27] A. Pocheville, "The ecological niche: history and recent controversies," in *Handbook of evolutionary thinking in the sciences*. Springer, 2015, pp. 547–586.

[28] H. Nguyen, C. Anderson, A. Trevor, A. Jain, Z. Xu, and C. C. Kemp, "El-e: An assistive robot that fetches objects from flat surfaces," in *Robotic helpers, int. conf. on human-robot interaction*, 2008.

[29] U.S. Dept. of Health and Human Services - Public Health Service, "Niosh work practices guide for manual lifting," Available at <https://www.cdc.gov/niosh/docs/81-122/pdfs/81-122.pdf> (2021/09/14), 1981.

[30] iRobot, "FACT SHEET: Roomba Intelligent FloorVac," Available at media.irobot.com (2021/09/13), 2002.

[31] A. R. Tilley, *The measure of man and woman: human factors in design*. John Wiley & Sons, 2002.

[32] V. Paquet and D. Feathers, "An anthropometric study of manual and powered wheelchair users," *International Journal of Industrial Ergonomics*, vol. 33, no. 3, pp. 191–204, 2004.

[33] F. Collins and M. Yim, "Design of a spherical robot arm with the spiral zipper prismatic joint," in *2016 IEEE international conference on robotics and automation (ICRA)*. IEEE, 2016, pp. 2137–2143.

[34] C. Mucchiani, S. Sharma, M. Johnson, J. Sefcik, N. Vivio, J. Huang, P. Cacchione, M. Johnson, R. Rai, A. Canoso, *et al.*, "Evaluating older adults' interaction with a mobile assistive robot," in *2017 IEEE/RSJ International Conference on Intelligent Robots and Systems (IROS)*. IEEE, 2017, pp. 840–847.

[35] J. J. Craig, "Introduction to robotics: mechanics and control," 2005.

[36] Y. S. Choi, T. Deyle, T. Chen, J. D. Glass, and C. C. Kemp, "A list of household objects for robotic retrieval prioritized by people with alz," in *2009 IEEE International Conference on Rehabilitation Robotics*. IEEE, 2009, pp. 510–517.

[37] S. Song, A. Zeng, J. Lee, and T. Funkhouser, "Grasping in the wild: Learning 6dof closed-loop grasping from low-cost demonstrations," *IEEE Robotics and Automation Letters*, vol. 5, no. 3, pp. 4978–4985, 2020.

[38] R. Munoz-Salinas, "Aruco: a minimal library for augmented reality applications based on opencv," *Universidad de Córdoba*, vol. 386, 2012.

[39] L. Kelley, K. Talke, P. Longhini, and G. Catron, "Tip-over prevention: Adaptive control development and experimentation," in *2015 IEEE International Conference on Robotics and Automation (ICRA)*. IEEE, 2015, pp. 4367–4372.

[40] E. Papadopoulos and D. A. Rey, "The force-angle measure of tipover stability margin for mobile manipulators," *Vehicle System Dynamics*, vol. 33, no. 1, pp. 29–48, 2000.

[41] M. Korayem, V. Azimirad, A. Nikoobin, and Z. Boroujeni, "Maximum load-carrying capacity of autonomous mobile manipulator in an environment with obstacle considering tip over stability," *The International*

Journal of Advanced Manufacturing Technology, vol. 46, no. 5-8, pp. 811–829, 2010.

- [42] M. J. A. Safar, K. Watanabe, S. Maeyama, and I. Nagai, “A study of tipping stability for omnidirectional mobile robot with active dual-wheel caster assemblies,” *Artificial Life and Robotics*, vol. 17, no. 1, pp. 145–151, 2012.
- [43] A. Jain, H. Nguyen, M. Rath, J. Okerman, and C. C. Kemp, “The complex structure of simple devices: A survey of trajectories and forces that open doors and drawers,” in *2010 3rd IEEE RAS & EMBS International Conference on Biomedical Robotics and Biomechatronics*. IEEE, 2010, pp. 184–190.
- [44] A. Jain and C. C. Kemp, “Improving robot manipulation with data-driven object-centric models of everyday forces,” *Autonomous Robots*, vol. 35, no. 2, pp. 143–159, 2013.
- [45] K. P. Hawkins, C.-H. King, T. L. Chen, and C. C. Kemp, “Informing assistive robots with models of contact forces from able-bodied face wiping and shaving,” in *2012 IEEE RO-MAN: The 21st IEEE International Symposium on Robot and Human Interactive Communication*. IEEE, 2012, pp. 251–258.
- [46] M. E. Cabrera, T. Bhattacharjee, K. Dey, and M. Cakmak, “An exploration of accessible remote tele-operation for assistive mobile manipulators in the home,” in *2021 30th IEEE International Conference on Robot & Human Interactive Communication (RO-MAN)*. IEEE, 2021, pp. 1202–1209.